ORIENTAL JOURNAL OF CHEMISTRY
An International Open Access, Peer Reviewed Research Journal
www.orientjchem.org
ISSN: 0970-020 X
CODEN: OJCHEG
2024, Vol. 40, No.(5):
Pg. 1460-1469

In-silico Designing and Synthesis of Small Molecule Potential Inhibitors of *Plasmodium falciparum* Plasmepsin I Based on HEA and Piperazine moieties

AMIT KUMAR GAUTAM[1], RUPINI BOYINA[2]*, ASHISH VERMA[3], SHIV GOVIND PRASAD[4], YASHVEER GAUTAM[5] and DEVENDRA PRATAP RAO[6]*

[1,3,6]Department of Chemistry, Coordination Chemistry Laboratory, Dayanand Anglo-Vedic (PG) College, Kanpur-208001, U.P., India.
[2]Department of Environmental Studies, SOITS, IGNOU, New Delhi-1100068, India.
[4]Department of Chemistry, Uttar Pradesh Textile Technology Institute, Kanpur-208001, India.
[5]Department of Chemistry, Pandit Prithi Nath (PG) College, Kanpur-208001, U.P., India.
*Corresponding author E-mail: devendrapratapprao@yahoo.com

http://dx.doi.org/10.13005/ojc/400529

(Received: July 20, 2024; Accepted: October 03, 2024)

ABSTRACT

Aspartic protease enzymes have been critical in the survival of *Plasmodium falciparum*. Catabolic degradation of hemoglobin plays a quintessential involvement in parasite life cycles and a digestive food vacuole plasmepsin I (*Pf*Plm I) was accessed as a possible drug target as a part of antimalarial drug discovery. Computational methods were utilized to navigate through a pool of HEA and Piperazine analogs to figure out the best hit out of the screened compounds. For further exploration, MD simulations were used on *Pf*PlmI-hit complexes to demonstrate their stability.

Keywords: Plasmepsin, Molecular docking, Simulation, HEA, Piperazine.

INTRODUCTION

Digestive food vacuole of *P. falciparum* remains equipped with four plasmepsins (*Pf*Plms) plasmepsin I, II IV & Histoaspartic protease (HAP), and they are essentially engaged in the catabolic degradation of hemoglobin during the course of intraerythrocytic cell cycle[1]. This study has been corroborated by hemoglobin hydrolysis by a naturally occurring pious enzyme. Malarial mortality remains a curse on humankind and a global escalation is witnessed in the highly affected regions of the African continent and South-East Asian region as supported by WHO and other public stake holding agencies[2,3]. WHO and other global agencies have been implementing several malaria-controlling programs, especially in the regions of high incidence but a reduction in malaria cases is yet to be seen[4]. Parasite resistance has been a stumbling block in the medical diagnosis of malaria and the development of potential therapeutic interventions is a pressing need[5].

Vaccine development remains a complex process and requires an integration of academia and industry over the period of time with a considerable influx of public funding meanwhile these small molecules can significantly contribute to controlling the parasite, responsible for millions of casualties globally. Availability of vaccines has added an effective arsenal to combat the deadly disease in the safeguard of people.

Two vaccines (RTS,S/AS01 & R21) are now available and being administered in African continent with varying efficacy to control malarial disease in children. Booster doses are a pivotal part of these vaccination programs as to complete the schedule of vaccine[6,7].

*Pf*plml and its digestive vacuole plasmepsins share 53–70% amino acid arrangements that match their expression pattern[8-10]. *Pf*Plm I is believed to contain a transmembrane domain at its N-terminus, encoding a polypeptide consisting of a 123 amino acid proregion and a 329 amino acid mature region. *Pf*Plm I appears to evolve a bilobal tertiary structure analogous to Pepsin based on sequence similarities with *Pf*Plm II and *Pf*PlmIV[11-14]. In line with current research on trophozoite immunolocalization within erythrocytes[15], once *Pf*Plm I reaches the parasite surface's double membrane, the zymogen matures into an enzyme in the digestive vacuole in conjugation with digested hemoglobin. Aspartic proteinase inhibitors Pepstatin A and SC-50083 both are effective against cultured *Pf*Plm I parasites[16,17]. Unlike Ro40–4388, Ro40–5576 and Ro40–5572 inhibit *Pf*Plm I with similar antiparasitic properties[17]. Ro40–4388 and Ro40–5576 have similar antiparasitic effects The development of new antimalarial drugs may be informed by these evidence sources, as *Pf*Plm I could potentially be a superior choice. Several studies have expressed the effectiveness of hydroxyethylamine (HEA) and piperazine as PfPlm binders[18-21]. Synthesis of HEA and piperazine analogs based on these findings were taken along to validate the present studies.

Methodology

Preparation of *Pf*Plml, ligand, and blind docking

The protein structure for *Pf*Plml (PDB: 3QRV) was accessed from (RCSB Protein Data Bank) and synthesized to remove structural defects in autodock vina[22]. Blind docking was executed instead of site-specific docking purposefully to get the desired results.

Molecular docking studies

PyRx was capitalized to perform blank molecular docking of the developed analogs on the line of Pepstatin inhibitors against *Pf*Plml.

Simulations of molecular dynamics

The docked complexes were simulated using molecular dynamics to demonstrate their dynamic behavior in the line of established bonafide control Pepstatin. Academic Maestro-Desmond simulations were conducted using the in-built OPLS-2005 force field[23-26]. Using the TIP3P water model, the docked complexes were solved in an orthorhombic box before simulation[27]. To neutralize the systems and maintain physiological pH, sodium ions (Na^+) and chlorine ions (Cl^-) were added. For all systems, an energetically minimization step at 100ps sustaining before simulation, all default conditions were conceived. The Nose–Hoover and Martyna–Tobias–Klein chain dynamic algorithms were utilized in the study, which was conducted at 1.0 bar and 300 K[28-29].

After following up all the requisite processes, two docked systems were produced within a time span of 100ns. *Pf*Plml retrieved the coordinates and energy at 20.0 and 20ps, respectively. RMSD, RMSF and protein-ligand interactions are used to assess docked complex stability. The stereo-chemical geometry of *Pf*Plm I was analyzed after MD simulation by Procheck[30,31].

Preparation of compound-1

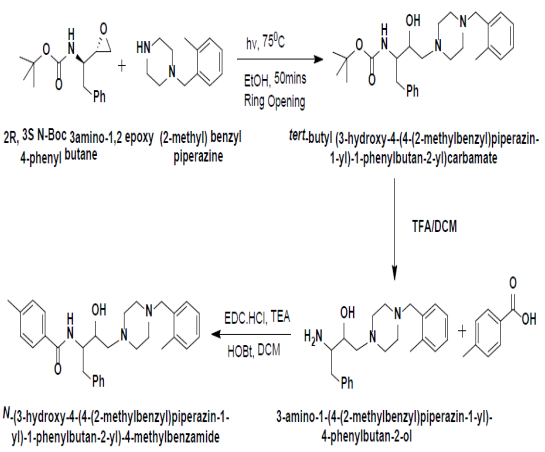

A 50 mL round-bottom flask was filled with N-Boc-3-amino-1,2-epoxy-4-phenylbutane (3.8 mmol) solvated in 5 mL ethanolic solution. Piperazine was then added as a second reactant, and the reaction mixture was subjected to microwave illuminated for a brief duration of 30 minute. at 300 W and 80°C. Removal of solvent was achieved under the vacuum condition after room temperature was attained by the reaction mixture. Recrystallized compound was accessed by employing ethyl acetate and hexane (1:9) mixture to proceed further. BOC deprotection was inevitable so was accomplished in the next step in a flask, with addition of dichloromethane, 20 mL volume capacity with an approximation of 3 mL trifluoracetic acid addition in a time consuming manner. As soon as the reaction was completed, additional solvents were expelled under vacuum conditions as the mixture was being stirred at RT. The addition of a base within the pH range of 8-9 modified the acidity level of the reaction mixture, which was subsequently extracted using $CH_3COOC_2H_5$ and rinsed with a brine solution. The compound layer was dried by the effective addition of anhydrous sodium sulfate, and the excess ethyl acetate was then removed under reduced pressure. Benzoic acid (2.0 mmol) and triethylamine (4.5 mmol) were combined in the presence of DCM (20 mL) were stirred at RT for approximately 30 mins with subsequent accretion of 1-Ethyl-3-(3-dimethylaminopropyl)carbodiimide (3.2 mmol). Hydroxyl benzotriazole (HOBt) (3.2 mmol) addition was accomplished at 0^0C and the intermediate (1.0 mmol) addition was achieved with ensured constant stirring. The final product was recovered by employing $CH_3COOC_2H_5$ (3x25 mL) once the process was completed in totality, and after that, the product was subjected to a vacuum to eliminate an additional amount of DCM solvent. Inevitably addition of anhydrous sodium sulfate was assured to fetch the water free organic layer followed by solvent elimination. Column chromatography (70: 30, hexane: ethyl acetate) was exercised to gain the finally purified product.

Spectroscopic data of compound 1: N-(3-hydroxy-4(4-(2-methylbenzyl)piperazin-1-yl)-1-phenylbutan-2-yl)-4-methylbenzamide

^{1}H NMR: δ 7.98 (d,1H), 7.74 (d,2H), 7.30 (s,2H), 7.17 (ddd,8H), 6.99 (d,1H), 4.30 (dd,1H), 4.01 (d,1H), 3.55 – 3.41 (m,2H), 3.19 – 2.80 (m,5H), 2.82 – 2.50 (m,5H), 2.36 (dd,8H) ($CDCl_3$, 400 MHz). ^{13}C NMR: δ 167.43, 142.09, 138.06, 137.63, 135.41, 131.33, 130.51, 129.94, 129.57, 129.27, 129.04–128.95, 128.70, 127.54, 127.22, 126.57, 125.71, 65.00, 60.52, 60.32, 53.76, 52.92, 50.97, 38.66, 29.78, 21.60, 19.24 ($CDCl_3$, 100 MHz).

Synthesis of compound 2

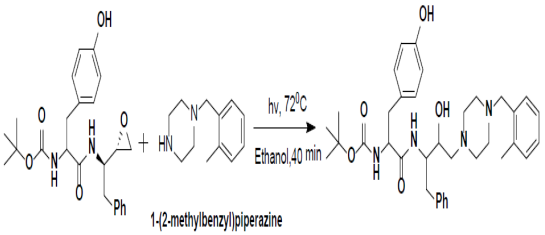

A round bottom flask with a 50 mL capacity was contaminated with 5.0 mmol of tert butyl(3-(4-hydroxyphenyl)-1-(methyl(1-(oxiran-2yl)-phenylethyl)amino)-1-oxopropan-2-yl)carabamate in 5 mL of ethanol followed by addition of 5.0 mmol of (2-methylbenzyl) piperazine and microwave irradiation was provided for a period spanning about 40 minutes. After that reaction mixture was subjected to vacuum to get rid of excess solvent followed by treatment of Ethyl acetate and hexane mixture to afford a recrystallized product.

Spectroscopic data of compound 2: t-butyl(1-((3-hydroxy-4(-4(2-methylbenzyl)piperazin-1-yl)-1-phenylbutan-2-yl)amino)3-(4-hydroxyphenyl)-1-oxopropan-2-yl)carbamate

^{1}H NMR (400 MHz, $CDCl_3$) δ 7.27–7.18 (m, 6H), 7.12 (s, 2H), 6.97 (d, 2H), 6.70 (d,2H), 6.52 (d,1H), 4.86 (s, 1H), 4.20 (s, 1H), 3.98 (dd, 8.0 Hz, 1H), 3.63 (d,1H), 3.43 (d,2H), 2.86 (d,4H), 2.46 (d,5H), 2.31 (s, 3H), 2.28–2.00 (m, 4H), 1.40 (s, 4H). ^{13}CNMR (100 MHz, $CDCl_3$) δ 171.36, 155.41, 138.03, 137.55, 135.99, 130.43, 130.38, 129.91, 129.51, 128.51, 127.75, 127.24, 126.53, 125.61, 115.88, 65.09, 60.62, 52.99, 38.94, 28.36, 19.33.

RESULT AND DISCUSSION

Targeting *Pf*Plm I has always been remarkable effects on parasite survival as degradation of complex protein, hemoglobin is critical for their survival during their life cycle in the human host. Designed analogs may have the capacity to inhibit *Pf*PlmI activity leading to parasite growth inhibition [30,31]. This key finding was an emboldened step and fuelled us to design and screen analogs aimed at *Pf*PlmI by deploying computational approaches.

Molecular docking studies

An analysis of molecular docking calculations was conducted investigate the potential HEA-piperazine analogs that could rope up effectively as part of its active site *Pf*Plm I enzyme using PyRx. Based on their computed binding affinity to the protein, docking scores (kcal.mol^{-1}) were used to evaluate and rank the poses of the ligands. Compared to pepsin, both compounds docked strategically within *Pf*Plm I's binding pocket. Compound I (C-I), Compound (C-II), and Pepstatin demonstrated docking scores of -8.4 kcal.mol^{-1}, -7.3 kcal.mol^{-1}, and -6.7 kcal.mol^{-1}, respectively. 2D-interaction plots of the docked candidates to PfPlm-I protein are depicted in Fig. 1. In the case of *Pf*Plm I-C1 complex, piperazine interacted with Asp 215 and Thr 218 by salt bridge and HG-bond, respectively. The p-methyl phenyl ring showed close interaction with Phe117 by virtue of hydrophobic interaction. Hydroxy group had great affinity to Asp32 by H-bond.1-benzhydryl substituted at pocket 2 interacted with Phe64 by means of pi-pi interaction (Figure 1a).

In *Pf*Plm I-C2 complex, Ser219 residue interacted to hydroxyl group, whereas Thr218 interacted to amine group. In *Pf*Plm I-control complex, control interacted to Ser219, Gly34, and asp215 by H-bond only. All three complexes were processed forward for MD simulation at 100ns to reveal their conformational stability as the docked ligand to the protein of interest.

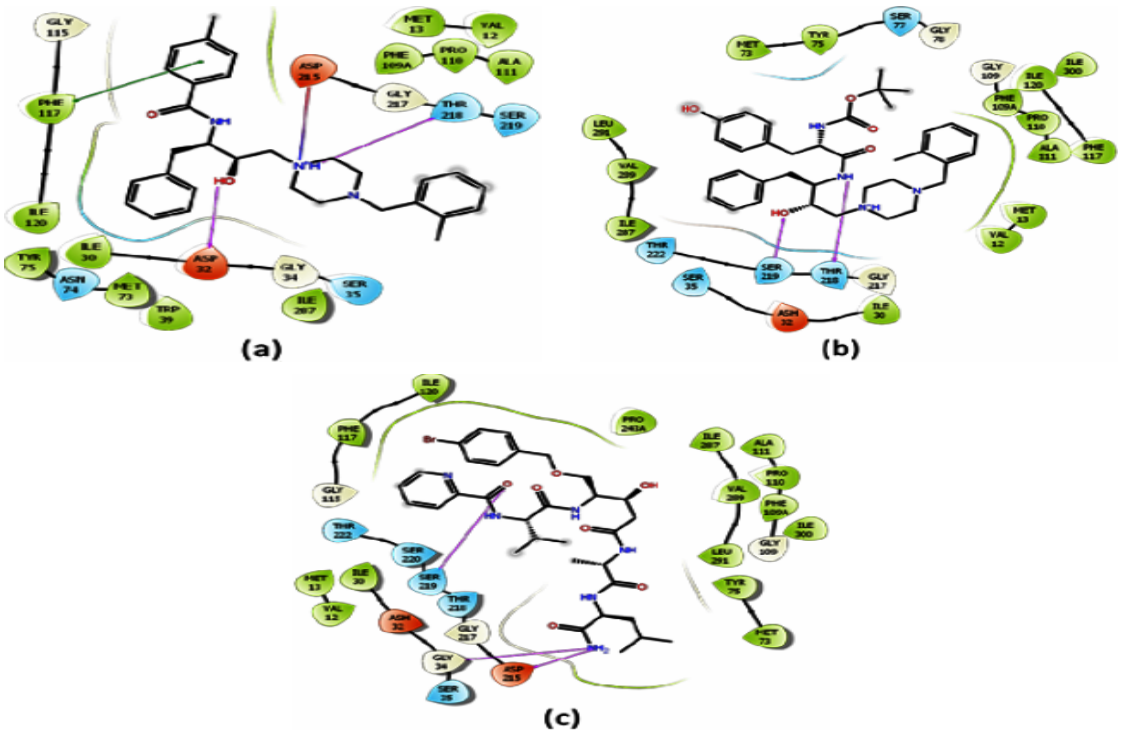

Fig. 1. Diagram illustrating interactions between ligand and residues comprising the binding site: (a) *Pf*Plm I-C1, (b) *Pf*Plm I-C2, and (c) *Pf*Plm I-Pepstatin complexes

MD simulations

Simulations of molecular dynamics were accelerated for both the compounds C1 and C2 at 100ns to unravel their stability and the conformational behavior in complex with *Pf*Plm I and compared with Pepstatin. As

a result of these simulations, the stability of these systems was determined. The C-*Pf*Plm I complex with C-1, C-2, and Pepstatin exhibited a stable RMSD plot within the first 10 nanoseconds, with fluctuations remaining within an acceptable range (≤3Å) (Fig. 2a, 3a, 4a). Averaging the RMSDC, $RMSD_{backbone}$, and $RMSD_{sidechain}$ values for *Pf*Plm I in complex with compound C1, the average values were 2.49, 2.49, and 3.62. Similarly, in compound C2, the average values of $RMSD_{C\alpha}$, $RMSD_{backbone}$, and $RMSD_{sidechain}$ for the *Pf*Plm I were 1.98 Å, 1.98 Å, and 2.42 Å, respectively. With compounds and Pepstatin, the average values of $RMSD_{C\alpha}$, $RMSD_{backbone}$, and $RMSD_{sidechain}$ for the *Pf*Plm I were 2.05 Å, 2.03 Å, and 3.33 Å, respectively. RMSD of C, backbone and sidechain of *Pf*Plm I in all three complexes were similar and reflected that protein was quite stable in character without any considerable conformational change in the structure of protein.

The average ligand RMSD fit on proteins of compound C1, C2, and Pepstatin were 5.17Å, 8.46 Å, and 2.97 Å, respectively as set out in Fig. 2a, 3a, and 4a. The RMSF plot indicated that the atoms of compound C-1 fluctuated below 2Å whereas tertiary-butyl group of C-2 was the highly fluctuated during the simulation.

As shown in Fig. 3c, compound C1 also interacts with residues of *Pf*Plm I's binding site. Compound C1 successfully upheld interactions with significant residues (Asp32, Phe117, and Asp215) and complement the molecular docking results. However, there were some additional interactions with residues such as Trp39, Phe109, and Ile120. Compound C2 in the first few nanoseconds interacted with Asp215, Phe117, and Tyr189, along with some other residues such as Asp290 as seen in Fig. 3c. We discovered that both ligands maintained interaction with catalytic residues compared to control (Figure 2c,3c,4c).

The number of contacts formed by C1, C2, and Pepstatin during the simulation is 10-11, 8-9, and 10-11, respectively (Figure 2d,3d,4d).

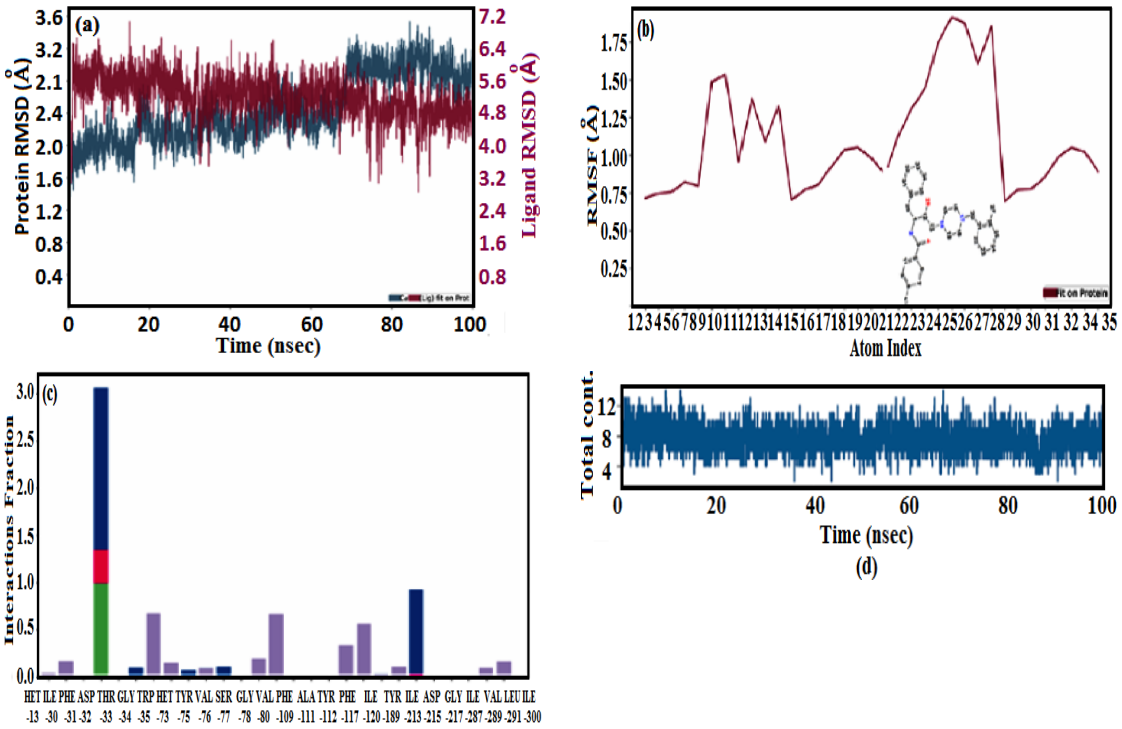

Fig. 2. MD results of *Pf*Plm I-C1 complex: (a) RMSD plot, (b) Ligand RMSF plot, (c) protein-ligand contacts histogram, (d) protein-ligand contacts timeline

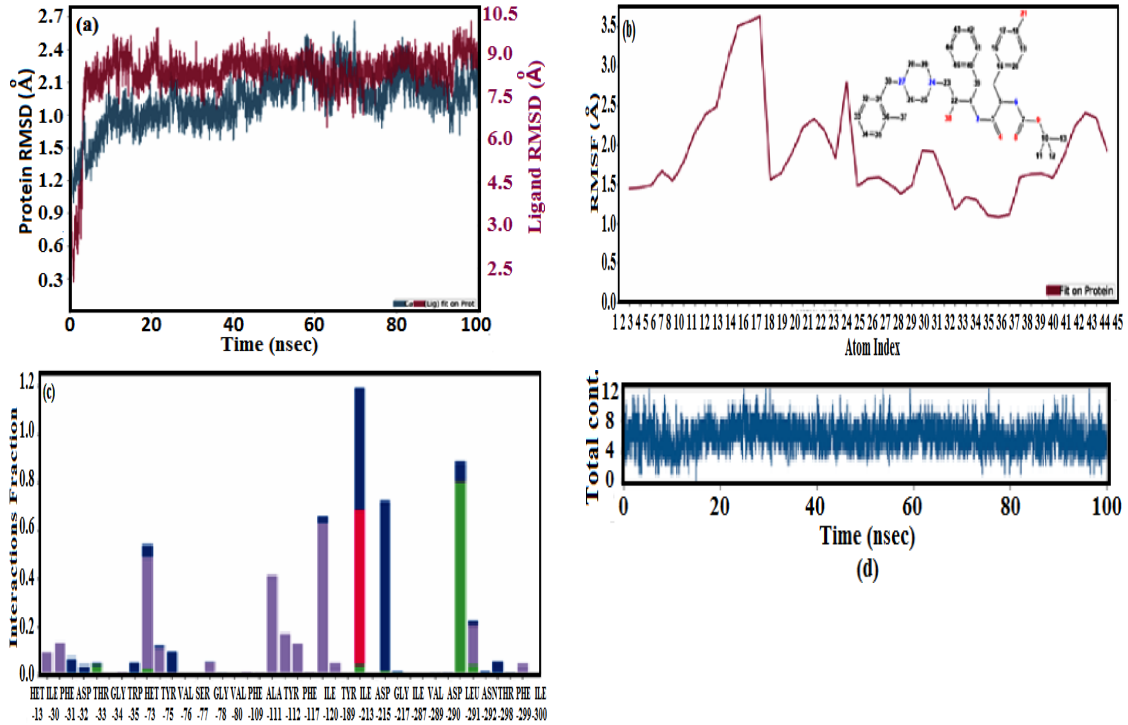

Fig. 3. MD results of *Pf*Plm I-C2 complex: (a) RMSD graph, (b) Ligand RMSF graph, (c) protein-ligand contacts histogram, (d) protein-ligand contacts timeline

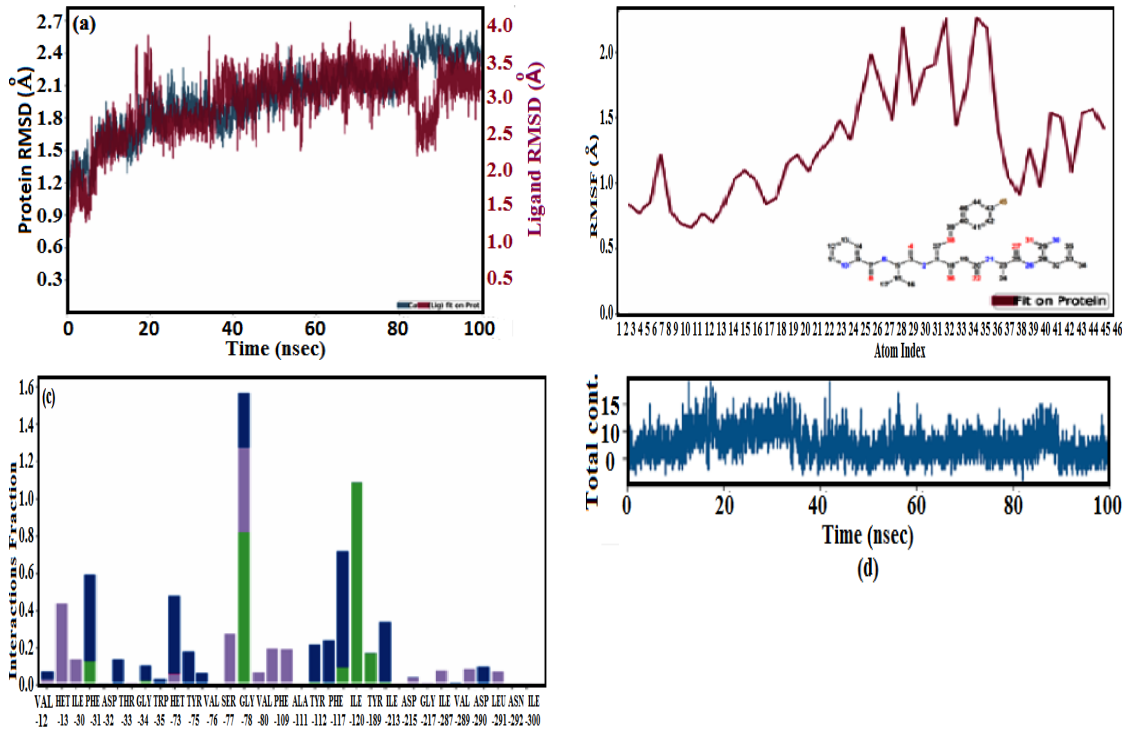

Fig. 4. MD results of PfPlm I-Pepstatin complex: (a) RMSD graph, (b) Ligand RMSF graph, (c) protein-ligand contacts histogram, (d) protein-ligand contacts timeline

Graph of Ramachandran plot from the last frame 100ns simulation for all three

complexes confirmed that the residues lie (≤ 1.1%) in the outlier region indicating a protein with good stereo-chemical geometry (Table 1 and Fig. 5; entry 1-3). The *Pf*Plm I-C1, and *Pf*Plm I-C2, possessed 2 (Val76, Ser77), and 2 (Val76, Asn11) residues respectively in the outlier region though no outlier residues were present for *Pf*Plm I-Pepstatin complex.

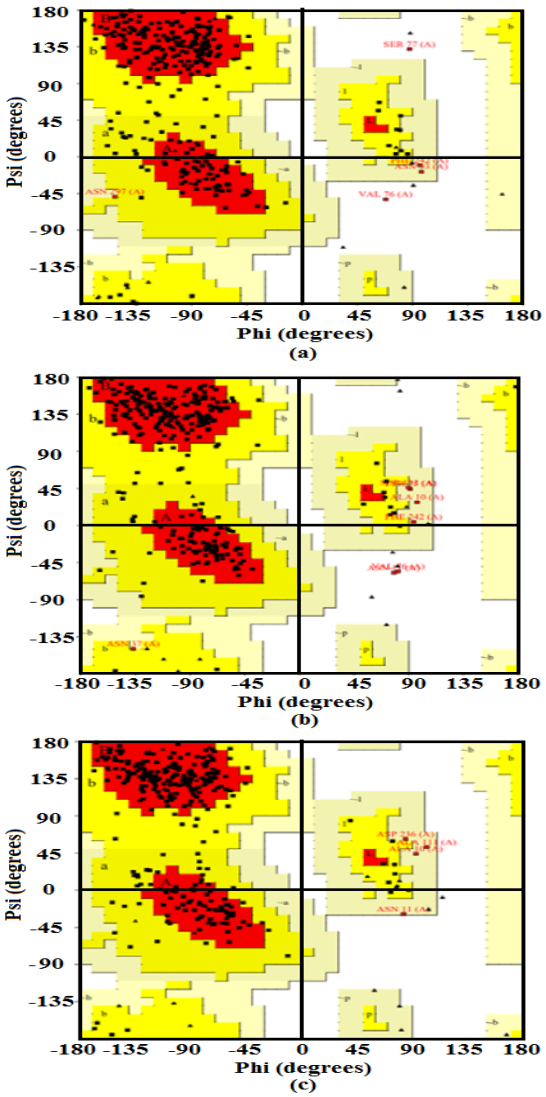

Fig. 5(a). Ramachandran plot of complex *Pf*Plml-C1, (b) Ramachandran plot of complex *Pf*Plml-C2 and (c) Ramachandran plot of complex *Pf*Plml-Pepstatin

Characteristics of ligands

Properties like ligand RMSD (ligand fit over ligand), MolSA, rGyr, PSA, intraHB, and SASA were utilized to elucidate the stability of compound C1, C2, and Pepstatin within *Pf*Plm I receptor complex as set out in Fig. 6a-c. Compound C1 showed ligand RMSD (ligand fit on ligand) within acceptable range whereas C2 showed slight high ligand RMSD (ligand fit on ligand) correlated to control in complex with *Pf*Plm I (Fig. 6). The radius of gyration and other parameters for C1 is similar compared to control whereas C2 showed slight high deviation as compared to control. MolSA, intraHB, PSA, rGyr, and SASA represent the molecular surface area, intramolecular H-bond, polar surface area, radius of gyration, and solvent accessible surface area, respectively.

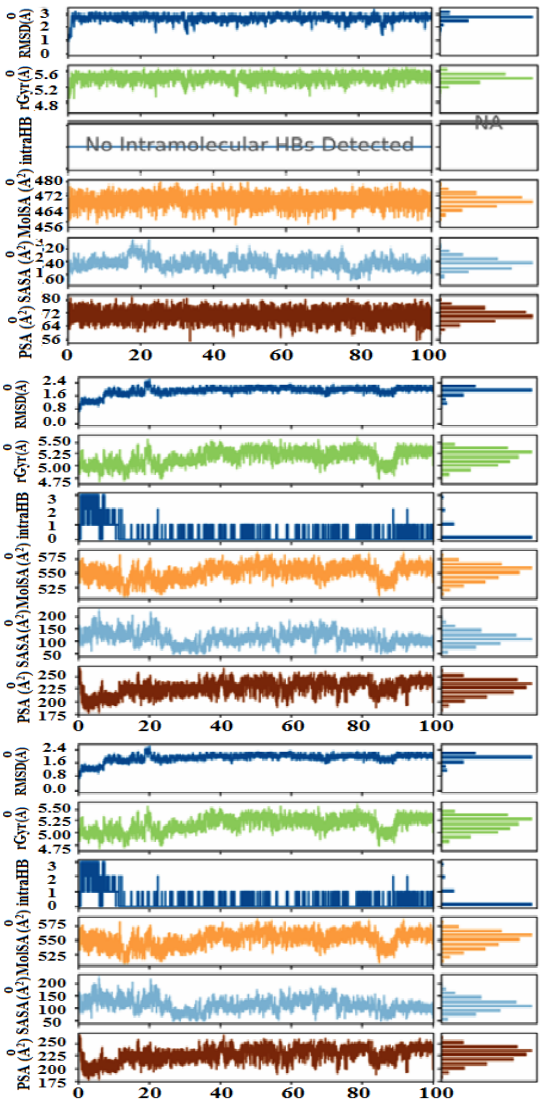

Fig. 6. Ligand properties during the 100ns simulations: (a) *Pf*Plml-C1 complex, (b) *Pf*Plml-C2 complex, and (c) *Pf*Plml-Pepstatin

Table 1: Ramachandran mapping of stereochemical geometry for residues of *Pf*Plml

Entry no	Complex	Residues number and % in Outlier region	Additional allowed region	Additional generously region	favoured region
1	*Pf*Plml-C1	2(0.7)	56(19.4)	3(1.0)	228(78.9)
2	*Pf*Plml-C2	2(0.7)	45(15.6)	5(1.7)	237(82.0)
3	*Pf*Plml-Pepstatin	0(0.0)	52(18.0)	4(1.4)	233(80.6)

CONCLUSION

Both compounds (C1 and C2) exerted their true docking score in comparison to potential inhibitor Pepstatin (-8.00 kcal.mol^{-1}). The stability of both compounds in complex with *Pf*Plm I was further validated by 100ns MD simulation, post-MD analyses followed by their result comparison with a notable inhibitor Pepstatin. The docking result of compound C1 (-8.4 kcal.mol^{-1}), and C2 (-7.3 kcal.mol^{-1}) was better in comparison of control (-6.7 kcal.mol^{-1}). MD results ascertained that compound C1 was very stable while C2 showed some fluctuations. Hence MD simulation evaluated compound C1 as a potential inhibiting agent of *Pf*Plm I.

ACKNOWLEDGMENT

The authors are grateful to the Department of Chemistry and the board of management at D.A-V. College, Kanpur, U.P., India, for providing infrastructure and other support to carry out the present studies.

Conflict of Interest: No

REFERENCES

1. Liu, P. Plasmepsin: Function, characterization and targeted antimalarial drug development. In: Natural remedies in the fight against parasites., **2017**, 183-218. https://doi.org/10.5772/66716.
2. Souza, M.C.; Padua, T.A.; Torres, N.D.; Costa, M.F.; Facchinetti, V.; Gomes, C.R.; Souza, M.V.; Henriques, M. Study of the antimalarial properties of Hydroxyethylamine derivatives using green fluorescent protein transformed Plasmodium berghei., *Mem. Inst. Oswaldo Cruz.*, **2015**, *110*(4), 560-565. https://doi.org/10.1590/0074-02760140466.
3. WHO: World Malaria Report. 2023. World malaria report **2023** (who.int)
4. Wells, T.N.C.; Alonso, P.L.; Gutteridge, W.E. New medicines to improve control and contribute to the eradication of malaria., *Nat. Rev. Drug Discov.*, **2009**, *8*, 879-891. https://doi.org/10.1038/nrd2972.
5. Dondorp, A.M.; Nosten, F.; Yi, P. Artemisinin resistance in plasmodium falciparum malaria. N., *Engl. J. Med.*, **2009**, *361*, 455-467. https://doi.org/10.1056/nejmoa0808859.
6. Schuerman, L. RTS, S malaria vaccine could provide major public health benefits., *The Lancet.*, **2019**, *394*, 735-36. https://doi.org/10.1016/s0140-6736(19)31567-3.
7. Mathenge, P.G.; Low, S.K.; Vuong, N.L.; Mohamed, M.Y.F.; Faraj, H.A.; Alieldin, G.I.; Khudari, R.Al.; Yahiaet, N.A. Efficacy and resistance of different artemisinin-based combination therapies: a systematic review and network meta-analysis., *Parasitol. Int.*, **2020,** *74*, 101919. https://doi.org/10.1016/j.parint.2019.04.016.
8. Banerjee, R.; Liu, J.; Beatty, W.; Pelosof, L.; Klemba, M.; Goldberg, D.E. Four plasmepsins are active in the plasmodium falciparum food vacuole, including a protease with an active-site histidine., *Proc. Natl. Acad. Sci.*, **2020**, *99*, 990-995. https://doi.org/10.1073/pnas.022630099.
9. Dame, J.B.; Yowell, C.A.; Omara-Opyene, L.; Carlton, J.M.; Cooper, R.A.; Li, T. Plasmepsin4 the food vacuole aspartic proteinase found in all plasmodium spp. Infecting man., *Mol. Biochem. Parasitol.*, **2003**, *130*, 1-12. https://doi.org/10.1016/s0166-6851(03)00137-3.
10. Liu, P.; Marzahn, M.R.; Robbins, A.H.; Gutierrez-de-Teran, H.; Rodriguez, D.; Mcclung, S.H.; Stevens, S.M.; Yowell, C.A.; Dame, J, B.; McKenna, R., Recombinant plasmepsin 1 from the human malaria parasite plasmodium falciparum: enzymatic characterization, active site inhibitor design, and structural analysis., *Biochemistry.*, **2009**, *48*, 4086-4099. https://doi.org/10.1021/bi802059r.

11. Asojo, E.; Afonina, S.V.; Gulnik, B.; Yu, J.W.; Erickson, R. Randad,; Madjahed, D.; Silva, A.M. Structures of Ser205 mutant plasmepsin II from plasmodium falciparum at 1.8 A in complex with the inhibitors rs367 and rs370. Acta Crystallographica section D., *Biological crystallography.*, **2002**, *58*, 2001-2008. https://doi.org/10.1107/s0907444902014695.
12. Asojo, O.A.; Gulnik, S.V.; E. Afonina, E.; Yu, B.; Ellman, J.A.; Haque, T.S.; A.M. Sila, T.S. Novel uncomplexed and complexed structures of plasmepsin II, an aspartic protease from Plasmodium falciparum., *J. Mol. Biol.*, **2003**, *327*, 173-181. https://doi.org/10.1016/S0022-2836(03)00036-6.
13. Clemente, J.C.; Govindsamay, L.; Madabushi, A.; S.Z. Fisher, R.E. Moose, C.A. Yowell, K. Hidaka, T. Kimura, Y. Hayashi, Y. Kiso. et.al. Structure of aspartic protease plasmepsin 4 from the malarial parasite Plasmodium malariae bound to an allophenylnorstatine-based inhibitor., *Acta Crysta.,* **2006**, *D62*, 246-252. https://doi.org/10.1107/s0907444905041260.
14. Silva, A.M.; Lee, A.Y.; Gulnik, S.V. et.al. Structure and inhibition of plasmepsin ii, a hemoglobin-degrading enzyme from plasmodium falciparum., *Proc. Natl. Acad. Sci.*, **1996**, *93*, 10034-10039. https://www.pnas.org/doi/pdf/10.1073/pnas.93.19.10034.
15. Francis, S.E.; Banerjee, R.; Goldberg, D.E. Biosynthesis and maturation of the malaria aspartic hemoglobinases plasmepsin I and II., *J. Biol. Chem.*, **1997**, *272*(23), 14961-14968. https://doi.org/10.1074/jbc.272.23.14961.
16. Francis, S.E.; Gluzman, I.Y.; Oksman, A.; Knickerbocker, A.; Mueller, R.; Bryant, M.L.; Sherman, D.R.; Rusell, D.G.; Goldberg, D.E. (1994) Molecular characterization and inhibition of plasmodium falciparum aspartic hemoglobinase., *The EMBO Journal.*, **1994**, *13*, 306-317. https://doi.org/10.1002/j.1460-2075.1994.tb06263.x.
17. Bailly, E.; Jambou, R.; Savel, J.; Jaureguiberry, G. Plasmodium falciparum: (1992) Differential sensitivity in vitro to E-64 (Cysteine Protease Inhibitor) and Pepstatin A (Aspartyl Protease Inhibitor)., *J. Protozool.*, **1992**, *39*, 593-599. https://doi.org/10.1111/j.1550-7408.1992.tb04856.x.
18. Moon, R.P.; Tyas, L.; Certa, U.; Rupp, K.; Bur, D.; Jacquet, C.; Matile, H.; Loetscher, H.; Grueninger-Leitch, F.; Kay, J. et al. Expression and characterization of plasmepsin I from Plasmodium falciparum., *Eur. J. Biochem.,* **1997**, *244*, 552-560. https://doi.org/10.1111/j.1432-1033.1997.00552.x.
19. Singh, A.K.; Rajendran, V.; Singh, S. et.al. Antiplasmodial activity of hydroxyethylamine analogs: Synthesis, biological activity and structure activity relationship of plasmepsin inhibitors., *Bioorg. Med. Chem.*, **2018**, *26*(13), 3837-3844. https://doi.org/10.1016/j.bmc.2018.06.037.
20. Singh, S.; Rajendran, V.; He, J.; Singh, A.K.; Achieng, A.O.; Pant. A.; Vandana.; Nasamau, A.S.; Pandit, M.; Singh, J. et. al. Fast acting molecules targeting malarial aspartic proteases, plasmepsin, inhibit, malaria infection at multiple stages., *ACS Infectious Diseases.*, **2019**, *5*, 184-198. https://doi.org/10.1021/acsinfecdis.8b00197.
21. Rao, D.P.; Yadav, H.S., Yadava, A.K.; Singh, S.; Yadav, U.S. Syntheses and spectroscopic studies on macrocyclic complexes of dioxomolybdenum(VI) with furil as precursor., *Journal of Chemistry.*, **2012**, *205123*, 7. https://doi.org/10.1155/2012/205123.
22. Bowers, K.J.; Chow, E.; Xu, H.; Dror, R.O.; Eastwood, M.P.; B.A. Gregersen, B.A.; Klepeis, J.L.; Kolossvary, I.; Moraes, M.A.; Sacerdoti, F.D.; Salmon, J.K.; Shan, Y.; Shaw. D.E.Scalable algorithms for molecular dynamics simulations on commodity clusters. In, Proceedings of the 2006 ACM/IEEE conference on Supercomputing. Tampa, Florida: Association for Computing Machinery., **2006**, 84–es. https://doi.org/10.1145/1188455.1188544.
23. Yadava, A.K.; Yadav, H.S.; Singh, Sanjay, Yadav, U.S.; Rao, D.P., Synthesis and characterization of some novel Schiff base complexes of oxovanadium(IV) cation., *Journal of Chemistry.*, **2013**, *689518*,5.https://doi.org/10.1155/2013/689518.
24. Jorgensen, W.L.; Tirado-Rives, J. The opls [optimized potentials for liquid simulations] potential functions for proteins, energy minimizations for crystals of cyclic peptides and crambin., *J. Am. Chem. Soc.*, **1988**, *110*, 1657-1666. https://doi.org/10.1021/ja00214a001.

25. Jorgensen, W.L.; Maxwell, D.S.; Tirado-Rives, J. Development and testing of the opls all-atom force field on conformational energetics and properties of organic liquids., *J. Am. Chem. Soc.*, **1996**, *118*, 11225-11236. https://doi.org/10.1021/ja9621760.
26. Jorgensen, W.L.; Chandrasekhar, J.; Madura, J.D.; Impey, R.W.; Klein, M.L. Comparison of simple potential functions for simulating liquid water., *J. Chem. Phys.*, **1983**, *79*, 926-935. http://dx.doi.org/10.1063/1.445869.
27. Martyna, G.J.; Tobias, D.J.; Klein, M.L. Constant pressure molecular dynamics algorithms., *J. Chem. Phys.*, **1994**, 101, 4177-4189. https://doi.org/10.1063/1.467468.
28. Nose, S. A unified formulation of the constant temperature molecular dynamics methods., *J. Chem. Phys.*, **1984**, *81*, 511-519. https://doi.org/10.1063/1.447334.
29. Laskowski, R.A.; MacArthur, M.W.; Moss, D.S.; Thornton, J.M. Procheck: A program to check the stereochemical quality of protein structures., *J. Appl. Cryst.*, **1993**, *26*, 283-291. https://doi.org/10.1107/S0021889892009944.
30. Daina, A.; Michielin, O.; Zoete.V. SwissADME: A free web tool to evaluate pharmacokinetics, drug-likeness and medicinal chemistry friendliness of small molecules., *Sci. Rep.*, **2017**, *7*, 42717. https://doi.org/10.1038/srep42717.
31. Cheuka, P.M.; Dziwornu, G.; Okombo, J.; Chibale, K. Plasmepsin inhibitors in antimalarial drug discovery: Medicinal chemistry and target validation (2000 to present)., *J. Med. Chem.*, **2020**, *63*, 4445–4467. https://doi.org/10.1021/acs.jmedchem.9b01622.